

Date of publication xxxx 00, 0000, date of current version xxxx 00, 0000.

Digital Object Identifier 10.1109/ACCESS.2017.Doi Number

USDE-based Continuous Sliding Mode Control for Quadrotor Attitude Regulation: Method and Application

LEXIU XU^{1,2,3}, XINGLING SHAO^{1,2,3} AND WENDONG ZHANG^{1,2,3}

¹Key Laboratory of Instrumentation Science and Dynamic Measurement, Ministry of Education, North University of China, Taiyuan 030051, China

²National Key Laboratory for Electronic Measurement Technology, North University of China, Taiyuan 030051, China

³School of Instrument and Electronics, North University of China, Taiyuan 030051, China

Corresponding author: Xingling Shao (shaoxl@nuc.edu.cn).

This work was supported in part by the National Natural Science Foundation of China under Grant 61603353 and Grant 61803348, in part by the Fund for the Shanxi 1331 Project Key Subjects Construction under Grant 1331KSC, in part by the Shanxi Province Science Foundation for Youths under Grant 201701D221123, and in part by the Scientific and Technological Innovation Programs of Higher Education Institutions in Shanxi.

ABSTRACT In this paper, an unknown system dynamics estimator (USDE)-based sliding mode control (SMC) is presented for quadrotor attitude tracking with the aims of conquering control oscillation problem and achieving great robustness. To enhance the anti-disturbance ability of quadrotors, the invariant manifold-based USDE, with features of simple structure and exponential error convergence, as well as low computational consumption, is introduced to recover the unknown disturbances by basic filter operation and algebraic calculation. Aiming at accelerating sluggish transient convergency in conventional disturbance compensation-based SMC, a novel quadrotor attitude SMC strategy containing a continuous double hyperbolic reaching law (DHRL) is designed, which greatly alleviates control oscillations without sacrificing dynamic response. The dramatical advantage of proposed scheme is that the chattering-free property and fast dynamic response with precise static tracking performance are simultaneously achieved. Meanwhile, all the error signals involved in the closed-loop system are proved to be bounded by Lyapunov analysis. Eventually, the effectiveness of explored control strategy is illustrated through simulations and experiments.

INDEX TERMS Chattering avoidance, sliding mode control, double hyperbolic reaching law, disturbance compensation, attitude tracking, quadrotors.

I. INTRODUCTION

In recent years, quadrotors have arisen extensive attentions from both industry and academic fields [1]-[5] owing to the unique characteristics such as rapid maneuverability, high agility and lowered complex structure. In pursuit of excellent performances, various studies on motion control of quadrotors have been conducted, containing path following [6], attitude tracking [7] and trajectory tracking [8]. Among which, attitude tracking is a fundamental topic especially for sophisticated missions including surveillance [9], transporting [10] and rescue [5]. However, because of the existence of inherent model nonlinearities, parametric uncertainties as well as extraneous wind disturbances, how to develop an effective attitude controller for quadrotors is still an ongoing issue in engineering practices. Focusing on this, abundant of innovative control policies have been conducted

for quadrotor attitude tracking, to name just a few, adaptive control [11]-[12], backstepping control [13], sliding mode control [14]- [15] and so on.

Due to the strong robustness and outstanding disturbance rejection, sliding mode control (SMC) has become a popular method for quadrotor operation [14]-[17]. However, it should be emphasized that the severe oscillations of SMC seriously affect its practical implementation. In order to cope with chattering problem, a great deal of scholars are devoted to devising improved SMC schemes, including but not being limited to adaptive SMC [18]-[19], terminal SMC [20] and disturbance compensation-based SMC [21]. An adaptive nonsingular SMC algorithm is investigated for quadrotor trajectory tracking [18]. By advancing an adaptive updating law to estimate the unknown upper bound of wind disturbance, an adaptive multivariable SMC is elaborated in

[19]. A terminal SMC scheme with the disturbance upper bound approximation is advanced, such that quadrotors can precisely track a time-varying trajectory with fast dynamic response [20]. In [21], a recurrent neural network (NN)-based SMC with small control gains is investigated for quadrotors to solve actuator fault problems. Among aforementioned schemes, the disturbance compensation-based SMC has been deemed as an attractive approach to tackle chattering issue. The mechanism of disturbance compensation-based SMC mainly lies in that a smaller switching gain value, merely required to be set larger than the upper boundary of disturbance estimation error instead of the disturbance upper bound, is endowed with the aid of disturbance estimate, leading to a smooth and continuous control action [39]. Certainly, the core point behind above-mentioned strategies is the selection of disturbance compensators. Up to now, abundant of disturbance estimators like extended state observer (ESO) [23], sliding mode observer (SMO) [25], function approximator-based techniques such as NN [26] and fuzzy logic systems [27] are exploited and incorporated with SMC design to circumvent the discontinuous control inputs. However, one should notice that for ESO [24] and SMO [25] designs requiring a series of calculations of derivative, a higher sensitivity to measurement noise is inevitably encountered. Meanwhile, as far as NN is concerned, it is still a nontrivial task to adjust suitable parameters to make weight updating converge within a finite time, and a heavy calculational cost is unavoidably incurred. More importantly, as smaller switching gains are permitted, continuous control behavior is attained by sacrificing dynamic response to some extent, i.e., satisfactory transient profile and control inputs cannot be synchronously assured for the available disturbance compensation-based SMC strategies [25]-[27].

Recently, unknown system dynamics estimator (USDE), elegantly proposed in [28] for robotic systems according to invariant manifold idea, is an efficient observer with a concise structure and low computational cost. With only filter operation and algebraic calculation, the lumped disturbances consisting of unmeasurable frictions, load variations and parametric uncertainties can be accurately estimated and compensated online by embedding USDE into controller design, endowing a robust tracking performance [32]. Such philosophy has also been successfully tailored for a hydraulic servo system [29] with less demanding computational cost. Thus, it is rewarding to practice an efficient quadrotor attitude control policy involved with USDE to facilitate practical implementation.

Motivated by above investigations, an USDE-based SMC with a double hyperbolic reaching law is developed to accelerate dynamic response and achieve reliable disturbance identification for quadrotor attitude tracking. The superiorities of proposed SMC can be summarized as follows: 1) Different from prevailing disturbance compensation-based SMC designs [21]-[26] for quadrotors suffering from

sluggish transient behaviors owing to the use of weak control gains, herein a novel double hyperbolic reaching law (DHRL) is developed by combining two different hyperbolic functions to accelerate the dynamic response without arising oscillation in quadrotor attitude control. By using a hyperbolic cosine function, a fast convergence rate is achieved when the sliding mode variable is far away from the switching surface. Moreover, with the aid of a hyperbolic tangent function, the sliding mode variable can infinitely approach to zero rather than crossing it, such that the unexpected oscillations will not be induced compared with prevailing exponential reaching law (ERL) [30] and power reaching law (PRL) [31].

2) Unlike previous disturbance compensation-based SMC for quadrotors using ESO [23] or SMO [25] exposed to high sensitivity to measurement noise, and NN-based observer [21][26] experiencing complexity parameter selection and heavy computational burden, here a preferable solution, USDE is adopted by imposing filtering operation upon the available system dynamics to reconstruct the unknown disturbances online. With the idea of invariant manifold, USDE with a straightforward structure is able to offer a reliable disturbance estimation based on [28], which consumes less computational resource than NN-based observers [35]-[38]. And an exponential estimation error convergence is assured by merely selecting one appropriate filter constant [32].

The rest of this paper is organized as follows. Section II provides the problem formulation and preliminaries. Section III gives the designs of the USDE, DHRL and controller with stability analysis, respectively. Both the simulation and experiment results with corresponding analyses are given in Section IV. Conclusion of this paper is drawn in Section V.

II. PROBLEM FORMULATION AND PRELIMINARIES

A. NOTATION

The following definitions are used throughout this paper. $[\cdot]^T$ stands for a column vector. $\text{diag}(\cdot)$ refers to a diagonal matrix. $|\cdot|$ represents the absolute value of a real number and $\|\cdot\|$ is the 2-norm of a vector or a matrix. $\mathbb{R}^{m \times n}$ is the set of real numbers with m and n being the number of rows and columns of \mathbb{R} , respectively.

B. MODEL OF QUADRTOR ATTITUDE SYSTEM

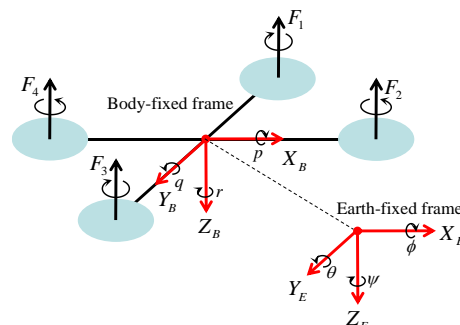


FIGURE 1. Illustration of quadrotors expressed by different frames.

Composed by a rigid cross frame and four rotors, the compact configuration of quadrotors is vividly depicted in Fig.1. Here, two coordinate frames, i.e., body-fixed frame and Earth-fixed frame, are defined to represent the attitude orientation of quadrotors, where Euler angles are expressed by the vector $\Theta = [\phi, \theta, \psi]^T \in \mathbb{R}^{3 \times 1}$ under Earth-fixed frame with ϕ , θ and ψ denoting the roll, pitch and yaw angle, respectively. And angular velocity vector under body-fixed frame is written in the form of $\Omega = [p, q, r]^T \in \mathbb{R}^{3 \times 1}$. Thrust force F_n ($n=1,2,3,4$) generated by the rotation of corresponding propeller, enables quadrotors to perform various attitude motions. Hence, the 3-DOF dynamic of quadrotor attitude system is formulated as

$$\begin{cases} \dot{\Theta} = \mathbf{W}\Omega \\ \mathbf{I}\dot{\Omega} = -\Omega \times \mathbf{I}\Omega + \mathbf{M} + \mathbf{D} \end{cases} \quad (1)$$

where $\mathbf{I} = \mathbf{I}^* + \Delta\mathbf{I} \in \mathbb{R}^{3 \times 3}$ is the unknown positive definite inertia matrix with $\mathbf{I}^* = \text{diag}(I_x^*, I_y^*, I_z^*) \in \mathbb{R}^{3 \times 3}$ and $\Delta\mathbf{I} \in \mathbb{R}^{3 \times 3}$ standing for the constant nominal rotational matrix and the uncertainty matrix of the rotational inertias. $\mathbf{M} = [M_1, M_2, M_3]^T \in \mathbb{R}^{3 \times 1}$ is deemed as the control torque vector. $\mathbf{D} = [D_1, D_2, D_3]^T \in \mathbb{R}^{3 \times 1}$ is the unknown disturbance vector caused by extrinsic wind gust. And \mathbf{W} is regarded as the transfer matrix from body-fixed frame to Earth-fixed frame, expressed by

$$\mathbf{W} = \begin{pmatrix} 1 & \sin\phi \tan\theta & \cos\phi \tan\theta \\ 0 & \cos\phi & -\sin\phi \\ 0 & \sin\phi \sec\theta & \cos\phi \sec\theta \end{pmatrix}$$

To facilitate subsequent analysis, here we define $\mathbf{x}_1 = \Theta = [x_{11}, x_{12}, x_{13}]^T \in \mathbb{R}^{3 \times 1}$ and $\mathbf{x}_2 = \dot{\Theta} = [x_{21}, x_{22}, x_{23}]^T \in \mathbb{R}^{3 \times 1}$, then (1) can be written in the following form:

$$\dot{\mathbf{x}}_2 = \underbrace{\mathbf{W}\Omega + \mathbf{W}(\mathbf{I}^*)^{-1}(-\Omega \times \mathbf{I}\Omega + \mathbf{D} - \Delta\mathbf{I}\dot{\Omega})}_{\mathbf{G}} + \underbrace{\mathbf{W}(\mathbf{I}^*)^{-1}\mathbf{M}}_{\boldsymbol{\tau}} \quad (2)$$

where $\mathbf{G} = [G_1, G_2, G_3]^T \in \mathbb{R}^{3 \times 1}$ is the vector of the lumped unknown disturbances and $\boldsymbol{\tau} = [\tau_1, \tau_2, \tau_3]^T \in \mathbb{R}^{3 \times 1}$ refers to the control input vector.

Assumption 1: Attitude information of quadrotors is measurable and conditions $\phi \in (-\pi/2, \pi/2)$, $\theta \in (-\pi/2, \pi/2)$ always hold.

Remark 1: All the attitude states and angular velocities can be directly measured by embedded inertial measurement units (IMUs) in our experiment platform. Additionally, the attitude motion of quadrotors is restrained physically because of the attachment to a universal joint, which is installed within an iron shelf, implying that \mathbf{W} is nonsingular all the time.

Control objective: This paper aims to exploring an USDE-based SMC scheme for quadrotor attitude system, enabling

1) The lumped disturbances encountered in quadrotor attitude control can be recovered online by USDE and the

estimation error is guaranteed to converge to a small set with an exponential rate.

2) All the error signals involved in closed-loop system can achieve ultimately uniformly bounded (UUB) stability and a satisfactory attitude tracking performance together with continuous control actions can be obtained.

III. CONTROLLER DESIGN

In this section, the USDE-based SMC involving a double hyperbolic reaching law will be designed for quadrotor attitude system (2) and corresponding control architecture is illustrated in Fig.2.

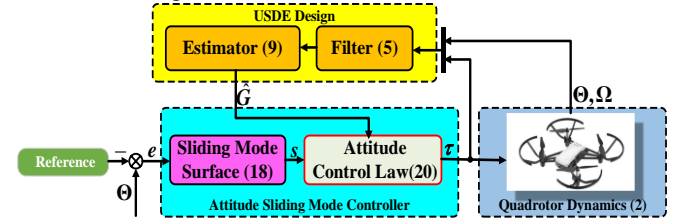


FIGURE 2. Architecture of presented control algorithm

A. USDE DESIGN

As the central part of disturbance compensation based-SMC, the disturbance estimator plays a prominent role in controller design. Different disturbance observers will bring different degrees of influences to control quality. For attitude dynamics of quadrotors (2), here enlightened by [28], the detailed construction process of USDE using simple filtering operation upon the available system dynamics is implemented to estimate the lumped disturbances.

Assumption 2 [29]: The lumped disturbance \mathbf{G} is continuous and differentiable, and there exists a positive constant g satisfying $\|\dot{\mathbf{G}}\| \leq g$.

Remark 2: In reality, the energy of wind gust is finite and the differentiation of attitude rates are bounded due to limited actuation ability, such that the variation of the angle and disturbance-related \mathbf{G} is continuous and bounded, thus *Assumption 2* is reasonable. In addition, one should note that the upper limit of the derivation of \mathbf{G} is only employed in stability analysis, instead of controller design.

Applying low-pass filter $(\cdot)^f = [\cdot]/(ks+1)$ on (2), we have

$$\frac{s}{ks+1}[\mathbf{x}_2] = \frac{1}{ks+1}[\mathbf{G}] + \frac{1}{ks+1}[\boldsymbol{\tau}] \quad (3)$$

where s denotes the differentiation operator and $k > 0$ is the filter time constant. Taking the inverse Laplace transform of (3), a filtered version of (2) can be obtained as follows:

$$\dot{\mathbf{x}}_2^f = \mathbf{G}^f + \boldsymbol{\tau}^f \quad (4)$$

where $\mathbf{x}_2^f \in \mathbb{R}^{3 \times 1}$, $\boldsymbol{\tau}^f \in \mathbb{R}^{3 \times 1}$ and $\mathbf{G}^f \in \mathbb{R}^{3 \times 1}$ represent the filtered \mathbf{x}_2 , $\boldsymbol{\tau}$ and \mathbf{G} respectively and fulfill

$$\begin{cases} k\dot{\mathbf{x}}_2^f + \mathbf{x}_2^f = \mathbf{x}_2, & \mathbf{x}_2^f(0) = 0 \\ k\dot{\boldsymbol{\tau}}^f + \boldsymbol{\tau}^f = \boldsymbol{\tau}, & \boldsymbol{\tau}^f(0) = 0 \end{cases} \quad (5)$$

Lemma 1: For quadrotor attitude dynamics (2) with auxiliary filtered variables (5), we consider the manifold

$\mathbf{Z} = (\mathbf{x}_2 - \mathbf{x}_2^f)/k - \boldsymbol{\tau}^f - \mathbf{G} = 0$ is an invariant manifold and one has $\lim_{k \rightarrow 0} \{\lim_{t \rightarrow +\infty} [(\mathbf{x}_2 - \mathbf{x}_2^f)/k - \boldsymbol{\tau}^f - \mathbf{G}]\} = 0$.

Proof: To prove the invariant manifold $\mathbf{Z} = 0$, here we construct a Lyapunov function as

$$V_z = \frac{1}{2} \mathbf{Z}^T \mathbf{Z} \quad (6)$$

Taking the derivative of \mathbf{Z} produces

$$\begin{aligned} \dot{\mathbf{Z}} &= (\dot{\mathbf{x}}_2 - \dot{\mathbf{x}}_2^f)/k - \dot{\boldsymbol{\tau}}^f - \dot{\mathbf{G}} = [\dot{\mathbf{x}}_2 - \frac{\mathbf{x}_2 - \mathbf{x}_2^f}{k} - (\boldsymbol{\tau} - \boldsymbol{\tau}^f) - k\dot{\mathbf{G}}]/k \\ &= -(\mathbf{Z} + k\dot{\mathbf{G}})/k \end{aligned} \quad (7)$$

Substiting (7) into the differentiation of V_z yields

$$\dot{V}_z = \mathbf{Z}^T \dot{\mathbf{Z}} = -\mathbf{Z}^T \mathbf{Z}/k - \mathbf{Z}^T \dot{\mathbf{G}} \quad (8)$$

According to Young's inequality, we have

$$-\mathbf{Z}^T \dot{\mathbf{G}} \leq \mathbf{Z}^T \mathbf{Z}/2k + k\dot{\mathbf{G}}^T \dot{\mathbf{G}}/2$$

And (8) can be rewritten in the following form:

$$\begin{aligned} \dot{V}_z &\leq -\mathbf{Z}^T \mathbf{Z}/k + \mathbf{Z}^T \mathbf{Z}/2k + k\dot{\mathbf{G}}^T \dot{\mathbf{G}}/2 \\ &\leq -\mathbf{Z}^T \mathbf{Z}/2k + k\dot{\mathbf{G}}^T \dot{\mathbf{G}}/2 \\ &\leq -V_z/k + kg^2/2 \end{aligned}$$

Integrating \dot{V}_z yields $V_z(t) \leq V_z(0)e^{-t/k} + k^2g^2/2$, which indicates that \mathbf{Z} is UUB and one can obtain $\|\mathbf{Z}\| = \sqrt{2V_z} \leq \sqrt{\|\mathbf{Z}(0)\|^2 e^{-t/k} + k^2g^2} \leq kg$, so we can confirm that $\lim_{k \rightarrow 0} \{\lim_{t \rightarrow +\infty} [\mathbf{Z}(t)]\} = 0$ is true, implying that $\mathbf{Z} = 0$ is an invariant manifold. ■

As a result, based on the relationship between the measurable dynamics and lumped disturbances, the USDE for quadrotor attitude control is designed as

$$\hat{\mathbf{G}} = \frac{(\mathbf{x}_2 - \mathbf{x}_2^f)}{k} - \boldsymbol{\tau}^f \quad (9)$$

with $\hat{\mathbf{G}} = [\hat{G}_1, \hat{G}_2, \hat{G}_3]^T \in \mathbb{R}^{3 \times 1}$ being the estimation of \mathbf{G} . And the estimation error vector is $\tilde{\mathbf{G}} = \mathbf{G} - \hat{\mathbf{G}} = [\tilde{G}_1, \tilde{G}_2, \tilde{G}_3]^T \in \mathbb{R}^{3 \times 1}$.

Theorem 1: For USDE (9), the estimation error $\tilde{\mathbf{G}}$ is ultimately uniformly bounded (UUB) and can converge with an exponential rate to a small set around zero, maintaining $\lim_{t \rightarrow +\infty} \|\tilde{\mathbf{G}}(t)\| = kg$.

Proof: Constructing a Lyapunov function as

$$V_1 = \frac{1}{2} \tilde{\mathbf{G}}^T \tilde{\mathbf{G}}$$

The differentiation of V_1 with respect to time t is

$$\begin{aligned} \dot{V}_1 &= \tilde{\mathbf{G}}^T \dot{\tilde{\mathbf{G}}} \\ &= \tilde{\mathbf{G}}^T (\dot{\mathbf{G}} - \dot{\hat{\mathbf{G}}}) = \tilde{\mathbf{G}}^T [\dot{\mathbf{G}} - (\dot{\mathbf{x}}_2 - \dot{\mathbf{x}}_2^f)/k + \dot{\boldsymbol{\tau}}^f] \end{aligned} \quad (10)$$

Combining (2) and (5), (10) can be rewritten as

$$\begin{aligned} \dot{V}_1 &= \tilde{\mathbf{G}}^T [\dot{\mathbf{G}} - (\mathbf{G} + \boldsymbol{\tau} - \dot{\mathbf{x}}_2^f - k\boldsymbol{\tau}^f)/k] \\ &= \tilde{\mathbf{G}}^T [\dot{\mathbf{G}} - (\mathbf{G} - \dot{\mathbf{x}}_2^f + \boldsymbol{\tau}^f)/k] \\ &= \tilde{\mathbf{G}}^T (\dot{\mathbf{G}} - (\mathbf{G} - \hat{\mathbf{G}})/k) = \tilde{\mathbf{G}}^T (-\tilde{\mathbf{G}}/k + \dot{\mathbf{G}}) \\ &= -\tilde{\mathbf{G}}^T \tilde{\mathbf{G}}/k + \tilde{\mathbf{G}}^T \dot{\mathbf{G}} \end{aligned} \quad (11)$$

By Young's inequality, $\tilde{\mathbf{G}}^T \dot{\mathbf{G}} \leq \tilde{\mathbf{G}}^T \tilde{\mathbf{G}}/2k + k\dot{\mathbf{G}}^T \dot{\mathbf{G}}/2$ can be derived. Thus, (11) can be deduced as

$$\begin{aligned} \dot{V}_1 &\leq -\tilde{\mathbf{G}}^T \tilde{\mathbf{G}}/k + \tilde{\mathbf{G}}^T \tilde{\mathbf{G}}/2k + k\dot{\mathbf{G}}^T \dot{\mathbf{G}}/2 \\ &\leq -\tilde{\mathbf{G}}^T \tilde{\mathbf{G}}/2k + k\|\dot{\mathbf{G}}\|^2/2 \\ &\leq -\tilde{\mathbf{G}}^T \tilde{\mathbf{G}}/2k + kg^2/2 \\ &\leq -V_1/k + kg^2/2 \end{aligned} \quad (12)$$

Consequently, a UUB stability can be reached for USDE (9). Integrating \dot{V}_1 , obviously we have the inequality $V_1 \leq V_1(0)\exp(-t/k) + k^2g^2/2$, such that estimation error can converge to a small residual set, expressed by

$$\|\tilde{\mathbf{G}}(t)\| = \sqrt{2V_1} \leq \sqrt{\|\tilde{\mathbf{G}}(0)\|^2 \exp(-t/k) + k^2g^2}$$

which implies that $\|\tilde{\mathbf{G}}(t)\| \rightarrow kg$ holds for $t \rightarrow +\infty$. And a quicker convergence together with a more precise estimate for USDE can be achieved by selecting a smaller k . ■

Remark 3: By applying USDE in SMC design, a smaller switching gain is allowable in parameter selection [39], then the oscillations of control signals can be suppressed without sacrificing anti-disturbance ability, achieving a high-accurate static attitude tracking. However, it should be stressed that although a chattering-free and robust control performance is realized, the transient response is weakened because of the small control gains, especially when the initial state is far away from the sliding mode surface. Thus, an innovative reaching law, which can provide an enhanced transient error convergence without evoking control chattering, will be elaborately tailored for USDE-based SMC to conquer such drawback.

B. DOUBLE HYPERBOLICAL REACHING LAW (DHRL) DESIGN

Inspired by the hyperbolic functions in terms of fast convergence, the double hyperbolic reaching law (DHRL) comprising of $\tanh(\bullet)$ and $\cosh(\bullet)$ is designed as

$$\dot{s}_i = -k_{1i} \tanh(as_i) - k_{2i} |s_i| \cosh(bs_i) \quad (13)$$

where s_i is the sliding mode variable; k_{1i} , k_{2i} , a and b are positive parameters; $\tanh(as_i) = (e^{as_i} - e^{-as_i}) / (e^{as_i} + e^{-as_i})$ denotes the hyperbolic tangent function and $\cosh(bs_i) = (e^{bs_i} + e^{-bs_i}) / 2$ refers to the hyperbolic cosine function.

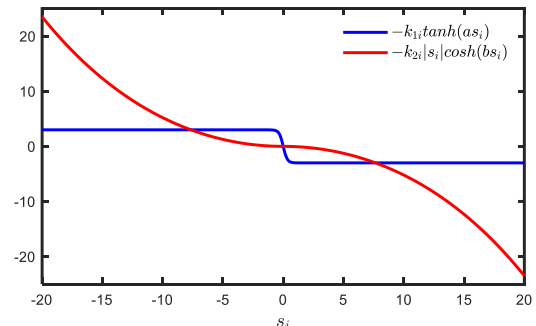


FIGURE 3. Different terms of proposed DHRL (13) with $a=0.1$, $b=0.05$, $k_{1i}=3$ and $k_{2i}=3$

From Fig.3, one can evidently find that when s_i is far away from the equilibrium point, $-k_{2i}|s_i|\cosh(bs_i)$ is large enough to make the sliding mode variable converge with a considerably rapid speed. When s_i approximate the

equilibrium point, the variation of s_i is mainly controlled by $-k_{1i} \tanh(as_i)$. The outstanding features of DHRL are that not only an accelerated convergence is guaranteed when the initial state is far away from zero, but also s_i can just approach the equilibrium point infinitely yet never reach or cross it, such that sudden chattering occurring in traditional RLs arising from $\text{sgn}(\cdot)$ function, will not be induced into control actions.

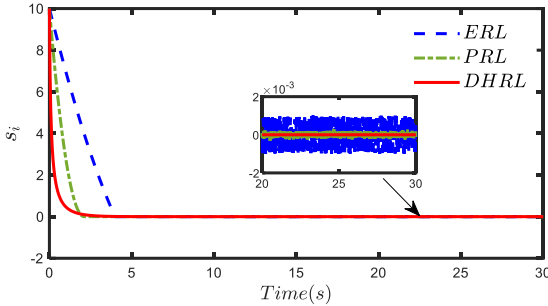


FIGURE 4. Simulation of different RLs

To further highlight the advantages of proposed double hyperbolic RL (DHRL), two prevailing reaching laws, i.e., exponential reaching law (ERL) [30] and power reaching law (PRL) [31] are employed to make a contrast. The ERL is given by $\dot{s}_i = -\kappa \text{sign}(s_i) / [\delta_0 + (1 - \delta_0)e^{-\alpha|s_i|^p}]$ with $\kappa = 3$, $\delta_0 = 0.5$, $\alpha = 2$ and $p = 2$. The PRL is in the form of $\dot{s}_i = -\kappa |s_i|^\gamma \text{sign}(s_i)$ and the parameters of PRL are $\kappa = 3$ and $\gamma = 0.5$. Parameters of DHRL are set as the same as Fig.2. All the initial values of sliding mode variables are set as 10.

As depicted in Fig.4, it can be easily found that DHRL has a faster and smoother converging curve. More importantly, the oscillation is also effectively alleviated in the steady-state phase, while the other two RLs can only converge to the equilibrium point with slower speeds and still suffer from the chattering problem when s_i is close to the equilibrium point.

Remark 4: Note that due to different structures of above RLs, it is impossible to make a completely fair comparison. However, by setting the similar switching gain values, the convergence performance of different RLs can be reflected to some extent.

Theorem 2: For DHRL (13), suppose a considerably small neighborhood $[0, \delta]$ with $0 < \delta < 1$. Once s_i enters it, s_i is considered convergent and convergence time of s_i is no more than $t_i = \ln[\sinh(a)/\sinh(\text{atanh}(k_{3i}/k_{1i}))]/(k_{1i}a) + 2(e^{s_{i0}} - e)/k_{2i}$ with k_{3i} representing the slope of s_i at the point of δ .

Proof: Suppose that s_i has a large positive initial value s_{i0} , the reaching time is

$$t_i = \int_{\delta}^{s_{i0}} \frac{1}{k_{1i} \tanh(as_i) + k_{2i}|s_i| \cosh(bs_i)} ds_i \quad (14)$$

Based on the analysis of (10), (11) can be rewritten as

$$\begin{aligned} t_i &= \int_{\delta}^{s_{i0}} \frac{1}{k_{1i} \tanh(as_i) + k_{2i}s_i \cosh(bs_i)} ds_i \\ &\leq \int_{\delta}^1 \frac{1}{k_{1i} \tanh(as_i)} ds_i + \int_1^{s_{i0}} \frac{1}{k_{2i}s_i \cosh(bs_i)} ds_i \end{aligned} \quad (15)$$

Here we define

$$\begin{cases} T_{1i} = \int_{\delta}^1 \frac{1}{k_{1i} \tanh(as_i)} ds_i \\ T_{2i} = \int_1^{s_{i0}} \frac{1}{k_{2i}s_i \cosh(bs_i)} ds_i \end{cases}$$

where T_{1i} is calculated as

$$\begin{aligned} T_{1i} &= \int_{\delta}^1 \frac{1}{k_{1i} \tanh(as_i)} ds_i = \int_{\delta}^1 \frac{\cosh(as_i)}{k_{1i} \sinh(as_i)} ds_i \\ &= \int_{\delta}^1 \frac{1}{ak_{1i} \sinh(as_i)} d(\sinh(as_i)) = \frac{1}{ak_{1i}} \ln(\sinh(as_i)) \Big|_{\delta}^1 \quad (16) \\ &= \frac{1}{ak_{1i}} \ln\left(\frac{\sinh(a)}{\sinh(\text{atanh}(k_{3i}/k_{1i}))}\right) \end{aligned}$$

Simultaneously, solving T_{2i} yields

$$\begin{aligned} T_{2i} &= \int_1^{s_{i0}} \frac{1}{k_{2i}s_i \cosh(bs_i)} ds_i = \int_1^{s_{i0}} \frac{2}{k_{2i}s_i (e^{bs_i} - e^{-bs_i})} ds_i \\ &< \int_1^{s_{i0}} \frac{2}{k_{2i}(e^{bs_i} - e^{-bs_i})} ds_i < \int_1^{s_{i0}} \frac{1}{k_2 e^{bs_i}} ds_i \quad (17) \\ &< \int_1^{s_{i0}} \frac{e^{-bs_i}}{k_2} ds_i \end{aligned}$$

Obviously, $T_{2i} < -(1/bk_{2i})e^{-bs_i} \Big|_1^{s_{i0}} = (e - e^{-bs_{i0}})/bk_{2i}$ is followed by (17). In conclusion, substituting (16) and (17) into (15) yields $t_i \leq T_{1i} + T_{2i} \leq \ln[\sinh(a)/\sinh(\text{atanh}(k_{3i}/k_{1i}))]/(k_{1i}a) + (e - e^{-bs_{i0}})/bk_{2i}$. And for $s_{i0} < 0$, the analysis is similar as above, so the detailed process for negative s_{i0} are omitted here. ■

Remark 5: For designed DHRL that using $\tanh(\cdot)$ rather than $\text{sgn}(\cdot)$, which can infinitely approach to zero but cannot cross it, the finite-time stability is hard to arrive because of asymptotic property within the boundary layer [33]-[34]. Thus, we introduce an auxiliary small set to approximate the fast convergence time.

C. USDE-based SMC DESIGN

Based on above theoretical analysis, an USDE-based SMC with the designed DHRL will be developed for quadrotor attitude tracking in this section.

To explore the controller, define attitude tracking error with the attitude command $\mathbf{x}_1^d = [x_{11}^d, x_{12}^d, x_{13}^d]^T \in \mathbb{R}^{3 \times 1}$ as

$$\mathbf{e} = \mathbf{x}_1 - \mathbf{x}_1^d = [e_1, e_2, e_3]^T \in \mathbb{R}^{3 \times 1}$$

The linear sliding mode surface is constructed as

$$s_i = \dot{e}_i + \mu_i e_i \quad (18)$$

where $\mu_i > 0 (i = 1, 2, 3)$ denotes a constant to be selected.

Taking derivative of s_i , we have

$$\begin{aligned} \dot{s}_i &= \ddot{e}_i + \mu_i \dot{e}_i = \ddot{x}_{2i} - \ddot{x}_{1i}^d + \mu_i \dot{e}_i \\ &= \hat{G}_i + \tau_i - \ddot{x}_{1i}^d + \mu_i \dot{e}_i \end{aligned} \quad (19)$$

Considering DHRL (13) and USDE design (5) and (9), the attitude control law τ_i is built as

$$\tau_i = \ddot{x}_{1i}^d - \mu_i \dot{e}_i - \hat{G}_i - [k_{1i} \tanh(as_i) + k_{2i}|s_i| \cosh(bs_i) + k_{3i}s_i] \quad (20)$$

where k_1 , k_{2i} and k_{3i} are all positive controller parameters set by users.

Theorem 3: For attitude dynamic of quadrotors (2), if the sliding mode variable is defined as (18), together with

attitude control law (20) and USDE design (5) and (9), supposing *Assumption 1* and *Assumption 2* are satisfied, then both of s_i and estimation error \tilde{G}_i are UUB.

Proof: The overall Lyapunov function is chosen as

$$V_2 = V_1 + \frac{1}{2} \sum_{i=1}^3 s_i^2$$

Differentiating V_2 along time yields

$$\dot{V}_2 = \dot{V}_1 + \sum_{i=1}^3 s_i \dot{s}_i = \dot{V}_1 + \sum_{i=1}^3 s_i (G_i + \tau_i - \ddot{x}_{li}^d + \mu_i \dot{e}_i) \quad (21)$$

Substituting the control law (20) into (21) produces

$$\begin{aligned} \dot{V}_2 &= \dot{V}_1 + \sum_{i=1}^3 s_i [\tilde{G}_i - (k_{1i} \tanh(as_i) + k_{2i} |s_i| \cosh(bs_i) + k_{3i} s_i^2)] \\ &= \dot{V}_1 + \sum_{i=1}^3 [s_i \tilde{G}_i - (k_{1i} s_i \tanh(as_i) + k_{2i} s_i |s_i| \cosh(bs_i) + k_{3i} s_i^2)] \\ &= \dot{V}_1 + \sum_{i=1}^3 [s_i \tilde{G}_i - (k_{1i} |s_i| \tanh(a |s_i|) + k_{2i} |s_i|^2 \cosh(b |s_i|) + k_{3i} s_i^2)] \end{aligned} \quad (22)$$

Using Young's inequality, one gets $s_i \tilde{G}_i \leq s_i^2/2 + \tilde{G}_i^2/2$ and \dot{V}_2 is deduced as

$$\begin{aligned} \dot{V}_2 &\leq \dot{V}_1 + \sum_{i=1}^3 [s_i^2/2 + \tilde{G}_i^2/2 - (k_{1i} |s_i| \tanh(a |s_i|) + k_{2i} |s_i|^2 \cosh(b |s_i|) + k_{3i} s_i^2)] \\ &\leq \sum_{i=1}^3 [s_i^2/2 + \tilde{G}_i^2/2 - (k_{1i} |s_i| \tanh(a |s_i|) + k_{2i} |s_i|^2 \cosh(b |s_i|) + k_{3i} s_i^2)] \\ &\quad - \tilde{G}^T \tilde{G} / 2k + kg^2/2 \\ &\leq \sum_{i=1}^3 [- (k_{3i} - 0.5) s_i^2] - \frac{(1/k-1)}{2} \tilde{G}^T \tilde{G} + kg^2/2 \\ &\leq - \sum_{i=1}^3 \frac{(2k_{3i}-1)}{2} s_i^2 - \frac{(1/k-1)}{2} \tilde{G}^T \tilde{G} + kg^2/2 \end{aligned} \quad (23)$$

Once $k_{3i} > 0.5$ and $0 < k < 1$ are fulfilled, \dot{V}_2 can be furtherly written in following form:

$$\dot{V}_2 \leq -\lambda^* V_2 + \zeta$$

with $\lambda^* = \min\{(2k_{3i}-1), (1/k-1)\} > 0$ and $\zeta = kg^2/2$. Solving \dot{V}_2 produces

$$V_2(t) \leq (V_2(0) - \frac{\zeta}{\lambda^*}) e^{-\lambda^* t} + \frac{\zeta}{\lambda^*} \leq V_2(0) e^{-\lambda^* t} + \frac{\zeta}{\lambda^*} \quad (24)$$

Therefore, it can be derived that both the sliding mode variable s_i and the estimation error \tilde{G}_i are UUB. Meanwhile, the boundedness of s_i also leads to a UUB result for e_i according to (18), such that all the error signals in closed-loop quadrotor attitude system are proved to be bounded. ■

Remark 6: To implement the designed control strategy, the controller parameters are needed to be well tuned. And some parameter tuning guidelines are summarized as follows:

1) Sufficiently large control gains k_{1i} , k_{2i} and k_{3i} are necessary to obtain fast attitude stabilization and satisfactory tracking accuracy. Nevertheless, overlarge magnitudes of control parameters may oscillate control inputs or even make them exceed actuator limits. Therefore, one should regulate proper control parameters to get a smooth and reliable attitude control performance.

2) The estimation accuracy of USDE mainly relies on the filter time constant k . Even though a small k can contribute to a fast estimation error convergence according to *Theorem 1*, the sensitivity to sensor noise of USDE will distinctly increase and unexpected oscillations might be induced, while a large k may cause sluggish estimate, thus a compromise should be made between system robustness and estimation error convergence.

IV. SIMULATIONS AND EXPERIMENTS

A. SIMULATION VALIDATION

TABLE 1. Parameters of presented control algorithm

Section	Values
DHRL	$a=3, b=0.1,$ $k_{11}=k_{12}=2.5, k_{13}=4, k_{21}=k_{22}=2, k_{23}=3$
USDE	$k=0.05$
Sliding mode controller	$\mu_1=\mu_2=\mu_3=2,$ $k_{31}=k_{32}=1, k_{33}=1.5$

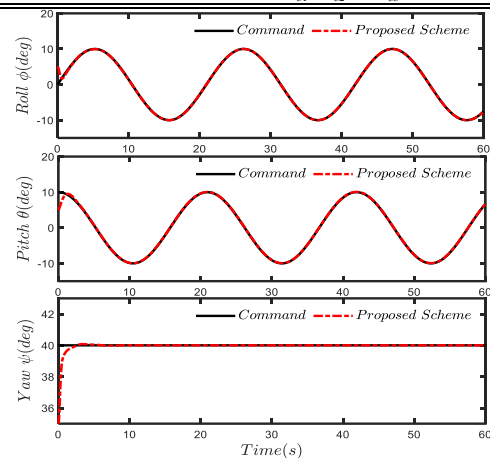


FIGURE 5. Attitude tracking performances in simulation

In this section, extensive numerical simulations are made to verify the effectiveness of presented algorithm. And the nominal inertia moments are $\mathbf{I}^* = \text{diag}(0.23, 0.21, 0.39) \text{kg} \cdot \text{m}^2$ with the uncertainties of rotational inertias being $\Delta \mathbf{I} = \text{diag}(0.032, -0.032, 0.096) \text{kg} \cdot \text{m}^2$. Then the initial values of Euler angles and angular rates are set as $\Theta(0) = [5, 5, 35]^T \text{deg}$ and $\Omega(0) = [0, 0, 0]^T \text{deg/s}$ respectively. $\mathbf{x}_1^d = [10 \sin(0.3t), 10 \cos(0.3t), 40]^T \text{deg}$ is selected as the attitude motion command with the time-varying external disturbance $\mathbf{D} = [1 + 0.5 \cos(2t), 1 + 0.4 \sin(t), 1 + \cos(1.6t)]^T \text{N} \cdot \text{m}$ being added. The simulation is conducted in MATLAB/Simulink platform with a fixed sampling time of 1 ms.

Using the parameters collected in TABLE 1, the simulation results are displayed in Figs.5-7. It is evident to see that the pre-given commands can be perfectly tracked under the premise of nonzero initial error, irrespective of the existence of unavailable wind disturbances and unknown system dynamics. In addition, fast dynamic tracking response is guaranteed by using the designed DHRL and input chattering can be avoided in control signals. Via selecting an

appropriate filter constant, the lumped disturbances can be precisely recovered by USDE online as depicted in Fig.7. As a result, by implementing USDE and DHRL in quadrotor attitude control, precise tracking performances, smooth control actions as well as excellent disturbance identification can be simultaneously provided without sacrificing dynamic response.

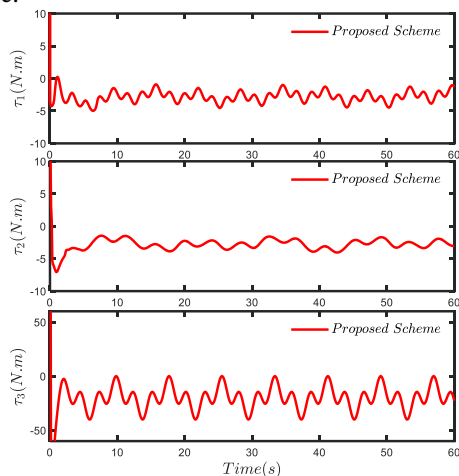


FIGURE 6. Control inputs in simulation

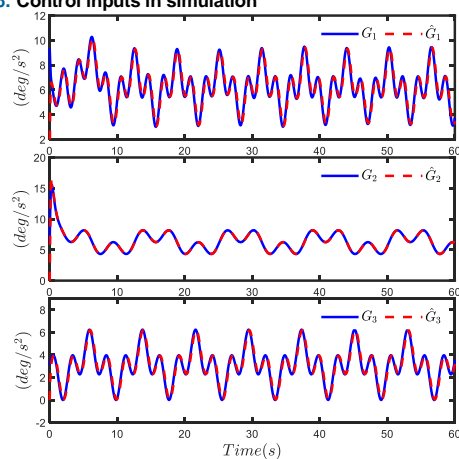


FIGURE 7. Disturbance estimation by USDE in simulation

B. COMPARISON SIMULATIONS

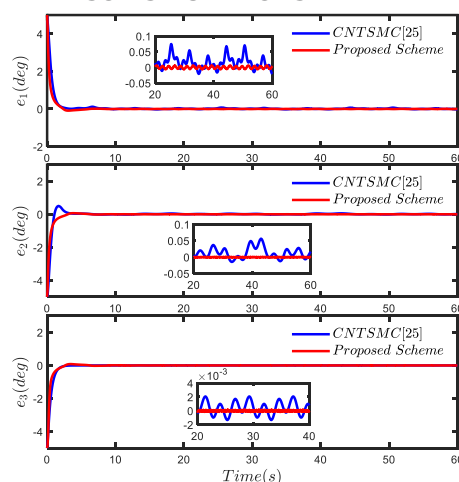


FIGURE 8. Attitude tracking comparison with CNTSMC [25] in simulation

To highlight the superiority of suggested control scheme, the related continuous nonlinear terminal SMC (CNTSMC) [25] is taken as a comparative object in this subsection. To make the comparison to be fair, the involved parameters are finely tuned to assure the identical convergence speeds. Tracking comparative results are shown in Figs.8-9 and TABLE 2 under the same disturbances. One can evidently find that even though both methods can accurately track the desired attitude commands regardless of the lumped disturbances, a more precise tracking performance offered by proposed scheme can be directly identified by the comparison of standard deviations, without introducing extra performance indices. A slight rapid dynamic response and decreased tracking deviation can be discerned. What is more, it is distinct to see that no matter in transient or static phase, in contrast to severe fluctuations appearing in CNTSMC, controlling oscillations are effectively accommodated with the help of USDE and devised DHRL, naturally yielding a reduced consumption in control efforts.

TABLE 2. Quantitative comparisons in simulation

	Index	CNTSMC [25]	Proposed Scheme
Steady error (Standard deviation)	e_1	0.3749	0.2739
	e_2	0.3741	0.2857
	e_3	0.3525	0.3093
Convergence time ^a	e_1	0.371s	0.278s
	e_2	0.331s	0.303s
	e_3	0.416s	0.337s
IAU ^b	τ_1	109.51	59.81
	τ_2	107.01	60.41
	τ_3	105.70	62.52
IADU ^c	τ_1	80.57	15.20
	τ_2	69.18	13.59
	τ_3	73.21	10.00

a. Convergence time refers to the first moment of tracking error entering the range (-2,2).

b. IAU represents integration of the absolute of control input.

c. IADU denotes the integration of the absolute value of difference between control input and its average.

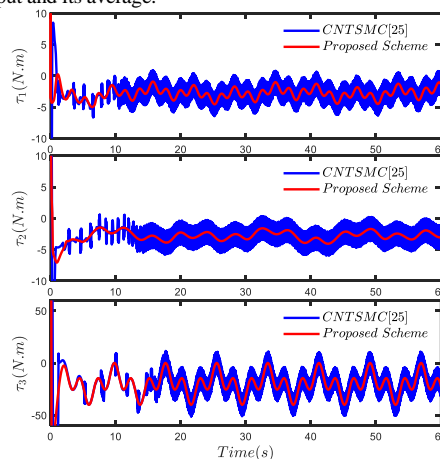


FIGURE 9. Control input comparison with CNTSMC [25] in simulation

Furthermore, to illustrate the advantages of USDE, the prevailing NN-based approximator [35] is introduced as a disturbance compensator to replace USDE while other units are kept unchanged. The comparison results are shown in Fig.10 and TABLE 3. One can find that even though both NN and designed USDE are capable of reconstructing the disturbances online, it is inferior in acquiring a rapid estimation for NN design due to the sluggish neural weight evolution. Next, quantitative comparison results in TABLE 3 have shown the superiority of USDE, demonstrating that a remarkable improvement in terms of tracking accuracy, convergence time as well as calculation cost is made, which is mainly originated from the straightforward structure of USDE with a simple parameter tuning, thus an affordable computational load can be desired for real-time application.

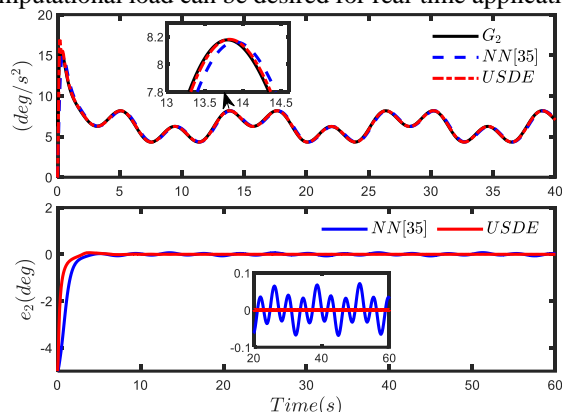


FIGURE 10. Comparison between NN [35]-based and USDE-based controllers

TABLE 3. Quantitative comparison between NN [35]-based and USDE-based controllers

Index		NN-based controller	USDE-based controller	Improvement
Steady error (Standard deviation)	e_2	0.527	0.289	-45.16%
Convergence time	e_2	1.09s	0.305s	-72.02%
Computational complexity ^d		22.5%	0.9%	-96%

d. Computational complexity is calculated by the ratio of summed computational time of controller to the whole running time, which is recorded by using the Tik/Tok program in MATLAB.

C. EXPERIMENTAL VALIDATION

To further demonstrate the feasibility of suggested controller, some validation experiments will be carried out based on the Links-UAV Testbench manufactured by Beijing Links Co., Ltd. The experiment setup and relationship between functional units are depicted in Figs.11-12. To acquire attitude states of quadrotors, two IMUs with a max sensitivity error of $\pm 3\%$, are equipped onboard to measure Euler attitudes and angular velocities. The onboard control computer, Pixhawk V3x is responsible for executing the designed control algorithm with a sampling time being 4ms

and generating pulse-width modulation (PWM) signals, which are sent to electronic speed controllers (ESCs) to drive the 4 propellers, such that desired control moments can be generated, allowing various quadrotor attitude motions. The monitoring computer accounts for arranging the attitude commands and transmitting them to Pixhawk V3x, while receiving state information of quadrotors and plotting the attitude tracking curves, which are all operated on MATLAB. All the signals between monitoring computer and Links-UAV Testbench are exchanged through a WIFI of 2.4Ghz. Additionally, to testify the robustness, a constant wind at the speed of 5m/s generated by an air blower is added as the external disturbance.

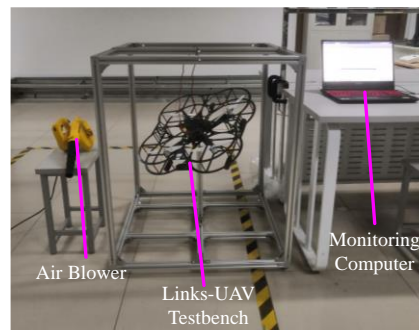


FIGURE 11. Experiment setup

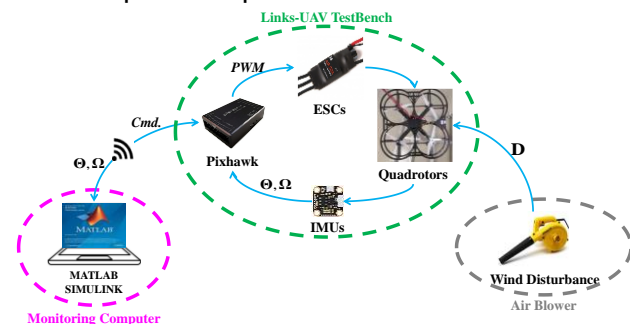


FIGURE 12. Relationship between functional units

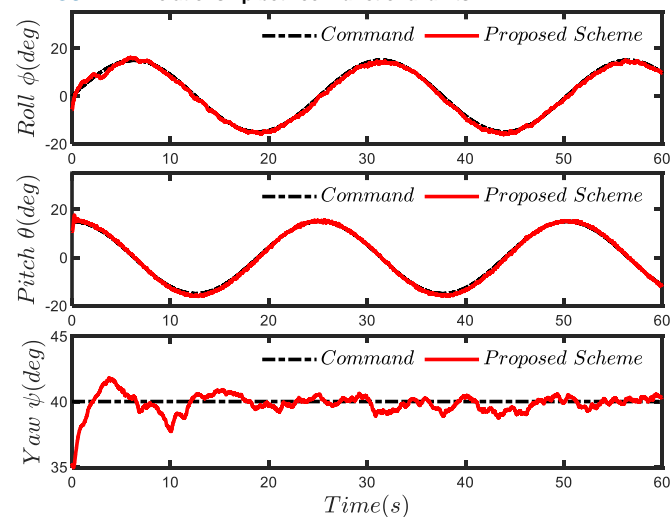


FIGURE 13. Attitude tracking in real-time application

The initial Euler angles and angular rates are selected as $\Theta(0) = [-5, 15, 35]^T$ deg and $\Omega(0) = [0, 0, 0]^T$ deg/s in the experiment. And the nominal rotational inertias are described

as $I_x^* = 0.023\text{kg}\cdot\text{m}^2$, $I_y^* = 0.021\text{kg}\cdot\text{m}^2$ and $I_z^* = 0.039\text{kg}\cdot\text{m}^2$, which are obtained by parameter identification algorithm. A larger attitude command, $x_1^d = [15\sin(0.3t), 15\cos(0.3t), 40]^T$ deg is set in experiment. Parameter selection of validation experiments is identical with TABLE 1 in simulation.

Experiment results are plotted in Figs.13-14. Apparently, the proposed method can produce a rapid and accurate attitude tracking behavior because of the contribution of DHRL and USDE. As shown in Fig.14, it is observed that continuous control actions can be calculated by proposed control scheme with a small degree of chattering phenomenon, which is reasonable since a low cost IMU is used to supply attitude measurements containing larger measurement noises. Certainly, an expensive IMU item will give rise to a higher precise attitude sensing and a noiseless control effort, thus a compromise should be made between implementation cost and tracking performance.

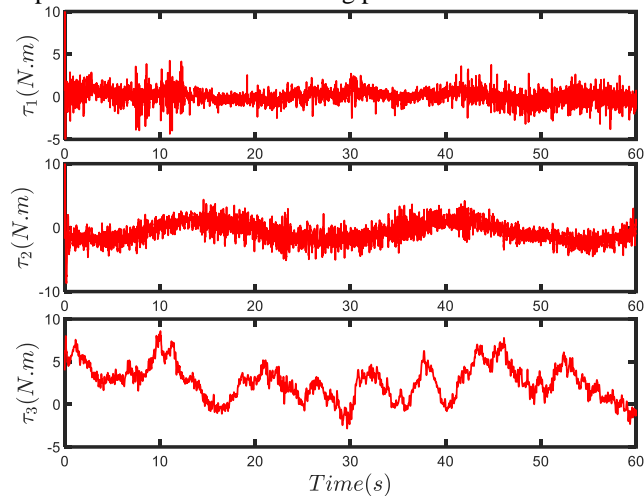


FIGURE 14. Control inputs in real-time application

D. EXPERIMENTAL COMPARISONS

To highlight the superiorities of the proposed control algorithm, two groups of comparative experiments are also carried out with CNTSMC developed in [25], whose parameters hold the same as previous simulation. To facilitate analysis, we choose the *Pitch* channel as the representative for comparison.

TABLE 4. Quantitative evaluation in Case 1

Index	CNTSMC [25]	Proposed Scheme	Improvement	
Steady error (Standard deviation)	e_2	1.66	0.54	-67.47%
Convergence time	e_2	1.116s	0.116s	-89.60%
IAU	τ_2	253.96	207.26	-18.34%
IADU	τ_2	190.58	168.17	-11.76%

Case 1: A time-varying signal $x_{12}^d = 15\cos(0.3t)$ is set as the command to testify the control performance. Contrasting results are shown in Fig.15 and TABLE 4. From these results, though both methods are able to provide a robust attitude tracking behavior under a time-varying command, the CNTSMC is deficient in achieving precise static tracking and smooth control actions. Conversely, by integrating the designed DHRL and USDE into SMC design, a better attitude tracking outcome with a higher accuracy, a rapid convergency and reduced chattering can be readily achieved under the significant wind gust.

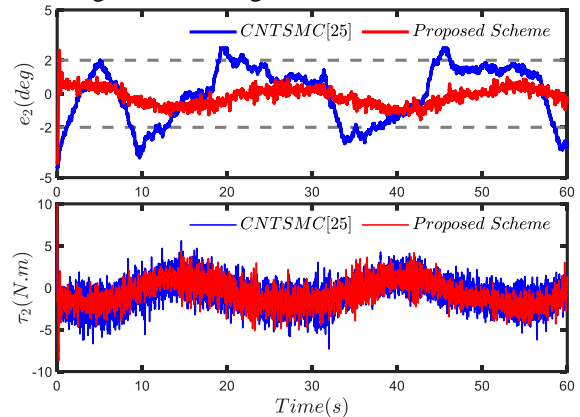


FIGURE 15. Experimental comparative result in Case 1

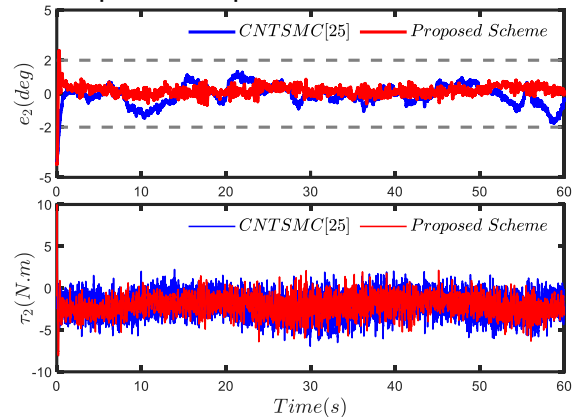


FIGURE 16. Experimental comparative result in Case 2

TABLE 5. Quantitative evaluation in Case 2

Index	CNTSMC [25]	Proposed Scheme	Improvement	
Steady error (Standard deviation)	e_2	0.614	0.332	-45.93%
Convergence time	e_2	0.336s	0.124s	-63.09%
IAU	τ_2	374.03	300.45	-19.67%
IADU	τ_2	294.14	252.13	-14.28%

Case 2: In this case, a step command, $x_{12}^d = 15$, is selected as the reference attitude motion. The corresponding results

are given in Fig.16 with quantitative indices shown in TABLE 5. From Fig.16, we can find that both CNTSMC and proposed scheme are capable of achieving a robust tracking performance, while a faster convergence with smaller tracking error is guaranteed by proposed control scheme. Besides, the chattering suppression of proposed scheme is also proved to be effective from the comparisons of IAU and IADU according to TABLE 5.

V. CONCLUSION

In this paper, a continuous USDE-based SMC consisting of a novel double hyperbolic reaching law is explored for quadrotor attitude control subject to unknown disturbance. Aiming at improving system robustness, an USDE with a straightforward structure and simple parameter adjustment, is employed to realize favorable identification of time-varying disturbances. To overcome the sluggish dynamic response caused by small control gains, a novel DHRL is devised with the combination of two different hyperbolic functions, assuring a fast convergence rate without inducing chattering phenomenon. Based upon above control design, simulations and experiments have been carried out together to demonstrate the salient features of proposed method and attained satisfactory results.

The following points will be pursued in future works. One is to derive a finite-time stability result rather than UUB result for USDE-based SMC design. Another is to generalize presented continuous SMC scheme to quadrotors with full dynamics.

REFERENCES

- [1] B. J. Guerreiro, C. Silvestre and Y. W. Cai, "LiDAR-based control of autonomous rotorcraft for the inspection of pierlike structures," *IEEE Trans. Con. Sys. Tech.*, vol. 26, no. 4, pp. 1430-1438, July. 2018.
- [2] L. Yang, B. Li and W. Li, "Concrete defects inspection and 3D mapping using CityFlyer quadrotor robot," *IEEE Journal. Autom. Sini.*, vol. 7, no. 4, pp. 991-1002, July. 2020.
- [3] R. G. Valenti, Y.-D. Jian, K. Ni and J. Xiao, "An autonomous flyer photographer," *Proc. IEEE Int. Conf. Cyber Technol. Autom. Control Intell. Syst. (CYBER)*, June. 2020.
- [4] S. K. Zhang, P. Chirarattananon, "Direct visual-inertial ego-motion estimation via iterated extended kalman filter," *IEEE Rob and Autom. Lett.*, vol. 5, no. 2, pp. 1476-1486, Apr. 2020.
- [5] T. Tomi, K. Schmid and P. Lutz, "Toward a fully autonomous UAV: research platform for indoor and outdoor urban search and rescue," *IEEE Rob & Auto. Mag.*, vol. 19, no. 3, pp. 46-56, Sep. 2012.
- [6] L. H. Qian and Hugh H. T. Liu, "Path-following control of a quadrotor UAV With a cable-suspended payload under wind disturbances," *IEEE Trans. Ind. Electron.*, vol. 67, no.3, pp.2021-2029, Mar. 2020.
- [7] K. Zhao, J. H. Zhang and D. L. Ma, "Composite disturbance rejection attitude control for quadrotor with unknown disturbance," *IEEE Trans. Ind. Electron.*, vol. 67, no. 8, pp. 6894-6903, Aug.2020.
- [8] B. Zhao, B. Xian and Y. Zhang, "Nonlinear robust adaptive tracking control of a quadrotor UAV via immersion and invariance methodology," *IEEE Trans. Ind. Electron.*, vol. 62, no. 5, pp. 2891-2902, May 2015.
- [9] P.S. Gohari, H. Mohammadi, S. Taghvaei, "Using chaotic maps for 3D boundary surveillance by quadrotor robot," *Appl. Soft Comput.*, vol. 76, pp. 68-77, Mar. 2019.
- [10] J. Wu, X. M. Chen, Q. J. Zhao, J. Li, and Z. G. Wu, "Adaptive neural dynamic surface control with prespecified tracking accuracy of uncertain stochastic nonstrict-feedback systems," *IEEE Trans. Cybernetics*, vol. pp, Aug. 2020.
- [11] R. Jiao, W. S. Chou, Y. F. Rong and M. J. Dong, "Anti-disturbance control for quadrotor UAV manipulator attitude system based on fuzzy adaptive saturation super-twisting sliding mode observer," *Appl. Sci-Basel.*, vol. 10, no. 11, Article ID 3719, Jun. 2020.
- [12] P. Cotaru, R. Edmonson and K. Sreenath, "Geometric L-1 adaptive attitude control for a quadrotor unmanned aerial vehicle," *J. Dyn. Syst-T. ASME.*, vol. 142, no.3, Article ID 031003.
- [13] L. X. Xu, H. J. Ma and D. Guo, "Backstepping sliding-mode and cascade active disturbance rejection control for a quadrotor UAV," *IEEE-ASME Trans. Mech.*, vol. 25, no.6, pp. 2743-2753, Dec. 2020.
- [14] G. Xu, Y. Q. Xia and D. H. Zhai, "Adaptive prescribed performance terminal sliding mode attitude control for quadrotor under input saturation," *Iet. Control Theory. A.*, vol. 14, no. 17, pp. 2473-2480, Nov. 2020.
- [15] A. Noordin, MAM. Basri and Z. Mohamed, "Adaptive PID controller using sliding mode control approaches for quadrotor UAV attitude and position stabilization," *Arab. J. Sci. Eng.*, vol. 46, no. 2, pp. 963-981, Jul. 2020.
- [16] JAC. Gonzalez, O. Salas-Pena and J. De Leon-Morales, "Observer-based super twisting design: A comparative study on quadrotor altitude control," *ISA Trans.*, vol. 109, pp. 307-314, Mar. 2021.
- [17] O. Bingol and H. M. Guzey, "Neuro sliding mode control of quadrotor UAVs carrying suspended payload," *Adv. Robotics*, vol. 35, no. 3-4, pp. 255-266, Jan. 2021.
- [18] M. Labbadi and M. Cherkaoui, "Robust adaptive nonsingular fast terminal sliding-mode tracking control for an uncertain quadrotor UAV subjected to disturbances," *ISA Trans.*, vol. 99, pp. 290-304, Apr. 2020.
- [19] B. L. Tian and J. Cui, "Adaptive finite-time attitude tracking of quadrotors with experiments and comparisons," *IEEE Trans. Ind. Electron.*, vol. 66, no. 12, pp. 9428-9438, Dec. 2019.
- [20] O. Mofid, S. Mobayen and WK. Wong, "Adaptive terminal sliding mode control for attitude and position tracking control of quadrotor UAVs in the existence of external disturbance," *IEEE ACCESS*, vol. 8, pp. 3428-3440, Jan. 2021.
- [21] B. Wang, Y. Y. Shen and Y. M. Zhang, "Active fault-tolerant control for a quadrotor helicopter against actuator faults and model uncertainties," *Aerosp. Sci. Technol.*, vol. 99, Article ID 105745, Apr. 2020.
- [22] M. A. Lotufo, L. Colangelo and P. M. Carlos, "UAV quadrotor attitude control: An ADRC-EMC combined approach," *Control. Eng. Pract.*, vol. 84, pp. 13-22, Mar. 2019.
- [23] C. L. Song, C. Z. Wei and F. Yang, "High-order sliding mode-based fixed-time active disturbance rejection control for quadrotor attitude system," *Electron.*, vol. 7, no. 12, Article ID. 357, Dec. 2018
- [24] X. L. Shao, X. H. Yue and J. Li, "Event-triggered robust control for quadrotors with preassigned time performance constraints," *Appl. Math. Comput.*, 2020, Doi: 10.1016/j.amc.2020.125667.
- [25] H. Ríos, R. Falcón and O. A. González, "Continuous sliding-mode control strategies for quadrotor robust tracking: real-time application," *IEEE Trans. Ind. Electron.*, vol. 66, no.2, pp. 1264-1272, Feb. 2019.
- [26] R. Garcia-Rodriguez and V. Parra-Vega, "A neuro-sliding mode control scheme for constrained robots with uncertain Jacobian," *J. Intell. Robot. Syst.*, vol. 54, no. 5, pp. 689-708, May 2009.
- [27] M. Zare, F. Pazoooki and SE. Haghghi, "Quadrotor UAV position and altitude tracking using an optimized fuzzy-sliding mode control," *Iete. J. Res.*, Doi: 10.1080/03772063.2020.1793694, Jul. 2020.
- [28] J. Na, B. R. Jing and Y. B. Huang, "Unknown system dynamics estimator for motion control of nonlinear robotic systems," *IEEE Trans. Ind. Electron.*, vol. 67, no. 5, pp. 3850-3859, May 2020.
- [29] J. Na, Y. P. Li, Y. B. Huang, G. B. Gao and Q. Chen, "Output feedback control of uncertain hydraulic servo systems," *IEEE Trans. Ind. Electron.*, vol. 67, no. 1, pp. 490-500, Jan. 2020.
- [30] C. J. Fallaha, M. Saad, H. Y. Kanaan, and K. Al-Haddad, "Sliding-mode robot control with exponential reaching law," *IEEE Trans. Ind. Electron.*, vol. 58, no. 2, pp. 600-610, Feb. 2011.
- [31] S. M. Mozayan, M. Saad, H. Vahedi, H. Fortin-Blanchette, and M. Soltani, "Sliding mode control of PMSG wind turbine based on enhanced

- exponential reaching law," *IEEE Trans. Ind. Electron.*, vol. 63, no. 10, pp. 6148-6159, Oct. 2016.
- [32] S. B. Wang, L. Tao and Q. Chen, "USDE-based sliding mode control for servo mechanisms with unknown system dynamics," *IEEE/ASME Trans. Mech.*, vol. 25, no. 2, pp. 1056-1066, Apr. 2020.
- [33] S. Yu, X. Yu, B. Shirinzadeh, and Z. Man, "Continuous finite-time control for robotic manipulators with terminal sliding mode," *Automatica.*, vol. 41, no. 11, pp. 1957-1964, 2005.
- [34] G. Bartolini, A. Ferrara, E. Usai, and V. I. Utkin, "On multi-input chattering-free second-order sliding mode control," *IEEE Trans. Autom. Control*, vol. 45, no. 9, pp. 1711-1717, Sep. 2000.
- [35] H. N. Si, X. L. Shao and W. D. Zhang, "MLP-based neural guaranteed performance control for MEMS gyroscope with logarithmic quantizer," *IEEE ACCESS*, vol. 8, pp. 38596-38605, 2020.
- [36] X. L. Shao, Y. Shi and W. D. Zhang, "Fault-tolerant quantized control for flexible air-breathing hypersonic vehicles with appointed-time tracking performances," *IEEE Trans. Aero. Elec. Sys.*, 2020, Doi: 10.1109/TAES.2020.3040519.
- [37] X. L. Shao, Y. Shi, W. D. Zhang and H. L. Cao, "Neurodynamic approximation-based quantized control with improved transient performances for MEMS gyroscopes: Theory and experimental results," *IEEE Trans. Ind. Electron.*, 2020, Doi: 10.1109/TIE.2020.3026297.
- [38] X. L. Shao, Z. B. Cao and H. N. Si, "Neurodynamic formation maneuvering control with modified prescribed performances for networked uncertain quadrotors," *IEEE. Syst. J.*, 2020, Doi: 10.1109/JSYST.2020.3022901.
- [39] J. X. Wang, L. Zhao and Y. Li, "Adaptive terminal sliding mode control for magnetic levitation systems with enhanced disturbance compensation," *IEEE Trans. Ind. Electron.*, vol. 68, no. 1, pp. 756-766, Jan. 2021.



LEXIU XU was born in Shandong, China, in 1999. He is pursuing the B.Sc. degree in electronic science and technology with the North University of China. His current interests include quadrotor attitude control and sliding mode control.



XINGLING SHAO received the M.S. degree in instrument science and technology from the North University of China, Shanxi, China, in 2012, and the Ph.D. degree in navigation, guidance and control from Beihang University, Beijing, China, in 2016. Since 2018, he has been a Professor with the Department of Instrument and Electronics, North University of China. His current research interests are in the elds of anti-disturbance control theory and application for nonlinear uncertain systems, advanced signal processing methods for navigation, and robust cooperative flight control theory and method for quadrotors.



WENDONG ZHANG was born in Henan, China in 1962. He is currently a Professor with the School of Instrument and Electronics, North University of China, Taiyuan, China. His research interest includes dynamics testing and control theory for nonlinear uncertain systems.